ISBN: 978-3-95450-262-2 ISSN: 2673-5350 doi: 10.18429/JACoW-IBIC2025-WEPMO30

DESIGN STUDY OF THE BEAM POSITION MONITOR FOR THE HADRON CENTER AT KUTAISI INTERNATIONAL UNIVERSITY*

Revaz Shanidze†
Kutaisi International University, Kutaisi Hadron Center, Kutaisi, Georgia

Abstract

Cyclotron-based proton beams are widely used in research and medical applications due to their capability to deliver bunched beams with a broad range of bunch charges. One of the most critical components in beam diagnostics is the beam position monitor (BPM), which must accurately measure the beam's position while minimizing disturbance to the beam.

At Kutaisi International University (KIU), a superconducting synchro-cyclotron (S2C2) provided by Ion Beam Applications (IBA) will be dedicated exclusively to research, supporting diverse experiments that benefit from proton bunched beams of different intensities. To accommodate these experiments, construction of compact beamline is planned.

In this work, we present the electromagnetic design study of an electrostatic BPM that can operate effectively and meet to the physical and operational constraints of the new beamline.

INTRODUCTION

The Beam Position Monitors (BPMs) are crucial diagnostic tools to effectively manipulate particle beams, by providing precise beam position. However, achieving sufficient signal levels from low-intensity bunched beams can be challenging. The minimum beam current for which a BPM yields usable position information (the detection threshold) is fundamentally limited by read-out electronic noise and manufacturing errors.

In the case of the IBA superconducting synchro cyclotron (S2C2) [1,2] at Kutaisi International University (KIU), the extracted proton beam consists of short pulses $\sim\mu s$ at a repetition rate of ∼1 kHz, main parameters of cyclotron are presented in the Table 1. The average extracted beam current is of the order of only a few tens of nano amperes. These parameters correspond to low bunch charges of the order of 10^{-11} to 10^{-10} C per pulse. Capacitive pickups (button-style BPMs) are a convenient choice for this application due to their simplicity, compactness, and ultrahigh vacuum compatibility. As a charged bunch passes, image charges are induced on the buttons, generating a voltage signal proportional to a fraction of the displacement and intensity of the beam. The fraction of the image current of the beam intercepted by a given button (and therefore the signal amplitude) depends on the electrode size, the position of the beam relative to it, and the transfer impedance [3].

This work, presents a simulation-based design study of a capacitive BPM for the S2C2 beamline at KIU. The goal is to determine the optimal button electrode size that yields the sufficient sensitivity to beam position across the expected range of bunch charges and offsets.

Table 1: General Parameters for IBA S2C2 [2]

Parameter	Description	Value
Size	yoke/pole radius	1.25 m/0.5 m
	weight	50 tons
Magnetic field	central/extraction	5.7 T/5.0 T
Beam pulse	rate/length	1000 Hz/7 μs
RF system	frequency	93-63 MHz
	voltage	10 kV
Maximum energy		250 MeV

General Considerations

An electrostatic monitor can typically be represented by an equivalent circuit that includes a current generator with the same value as the fraction of intercepted image current, which is then shunted by the electrode capacitance to ground. To connect the button to the detector circuit, a short length of modified coaxial cable with a characteristic impedance of R_0 is used, and an R_0 resistor terminates it.

It is worth noting that the circuit model delivers satisfying results with only minor corrections necessary for a circular button geometry and relativistic beam velocities, i.e., TEM-like (transverse electromagnetic) field pattern. If the beam is accelerated to a non-relativistic velocity, $\beta \ll 1$, as for cyclotrons, the electric field cannot be described by a TEM wave anymore. Instead, the field pattern has a significantly longitudinal extension because the electric field propagation is faster than the beam velocity [4]. However, for higher beam velocities, i.e., for $\beta \geq 0.3$, the electric charge distribution squeezes approaching a layer TEM wave, so the circuit model should provide good approximation in our case [5,6].

When the beam is centered, the transfer impedance, which is the complex ratio of the voltage induced by the beam at the external termination to the beam current, can be expressed as:

$$Z_b(\omega) = \phi R_0 \left(\frac{\omega_1}{\omega_2}\right) \frac{j\omega/\omega_1}{1+j\omega/\omega_1}\,, \qquad (1)$$

here, by the frequencies ω_1 and ω_2 represent: $\omega_1 = 1/R_0C_b$ and $\omega_2 = c/2r$, where C_b is the button capacitance to ground, r is the radius of the button, c is the speed of light, and b is the radius of the beam pipe. The coverage factor, ϕ, is also defined in terms of r and b, as $\phi = r/4b$ [7].

* The work has been supported by the Shota Rustaveli National Science Foundation of Georgia: SRNSFG grant No. FR-22-8306.
† revaz.shanidze@kiu.edu.ge

ISBN: 978-3-95450-262-2 ISSN: 2673-5350 doi: 10.18429/JACoW-IBIC2025-WEPMO30

The absolute value of the transfer impedance,

$$|Z_b(\omega)| = \phi R_0 \left(\frac{\omega_1}{\omega_2}\right) \frac{\omega/\omega_1}{\sqrt{1+(\omega/\omega_1)^2}} \quad , \qquad (2)$$

increases quadratically with the button radius, making a larger radius preferable for higher sensitivity across all frequencies. Enhancing the electrode surface improves the overall response, but increasing capacitance reduces the response at high frequency, while decreasing capacitance has the opposite effect. To reduce the low-frequency corner of the differentiator response, the load resistor value must be increased. However, these parameters are interdependent, increasing the radius may result in a linear or quadratic increase in capacitance, depending on the design. It is not feasible to increase the button radius beyond a certain limit, as the longitudinal coupling impedance scales as r^4,

$$Z_l(\omega) = \phi \left(\frac{\omega_1}{\omega_2}\right) Z_b \quad . \qquad (3)$$

The expression underestimates the coupling impedance, as it only considers the fields that contribute to the output signal formation. Numerical simulations have revealed other modes that do not dissipate their power in the external termination, such as the TE_{11}-like mode (transverse electric), which has a wavelength close to the mean perimeter of the annular cut created by the button and beam pipe walls. A smaller button radius is required to shift the frequency of the first parasitic mode towards higher frequencies, avoiding high power losses in the button BPM. The annular cut also contributes to the coupling impedance, which can be estimated analytically at low frequencies,

$$Z_{lcut}(\omega) = j \frac{Z_0 \omega (r+w)^3}{8cb^2\{ln[32(r+w)/w]-2\}} Z_{lcut} \quad . \qquad (4)$$

The coupling impedance is heavily dependent on the button radius, as evidenced by Eq. (4), where Z_0 represents the free space impedance, and by w size of the gap between the button and vacuum chamber wall is denoted.

MODELLING AND SIMULATIONS

Each button electrode has a of 14 mm radius at the annular cut with the vacuum chamber and a of 1 mm gap with the beampipe wall. The bunch length used in the wakefield simulations is 30 mm traveling along the structure's central axis. The BPM coaxial parts match the impedance of a 50 Ω. A glass ring for vacuum insulation is located near the button region. It has a dielectric constant of about 6.

In the wakefield calculation, a Gaussian beam is introduced in the z-direction, leading to the generation of electromagnetic fields at the BPM structure [8]. To prevent the reflection of electromagnetic waves at the beam entrance and exit planes, waveguide boundary conditions are imposed.

To evaluate the coupling impedance of a button, one can either use the wakefield or its Fourier transform. The latter allows us to identify potential resonant modes that the particle bunch excites in the BPM. The resolution of narrow resonances in the impedance spectrum is directly proportional to the number of sampling points used in the wakefield calculation [9]. Therefore, we compute the wakefield up to s = 3 m, where s represents the bunch coordinate.

In order to estimate the transfer and coupling impedance of the button we have simulated structure also with the measurement method based on a coaxial wire put along with the beam tube.

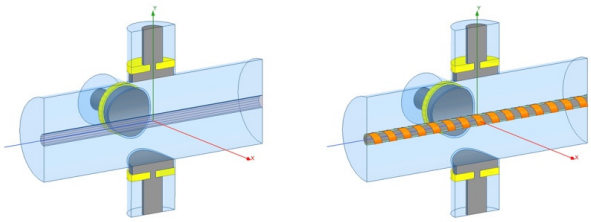

Figure 1: Left: wire structure, Right: helix structure.

Figure 1 displays the geometries used in the simulations to calculate the S-parameters. Two different methods were employed: simulations with only wire and with wire that is wrapped by conducting helix, to mimic the lower beta field patterns [10]. The transfer impedance vs frequency can be found from the values of the scattering matrix elements. By computing the transfer impedance at the coaxial line port as a function of frequency, we can determine the signal strength picked up by the BPM as the beam traverses the corresponding section of the vacuum chamber [11, 12].

RESULTS

Figure 2 presents comparison of the transfer impedance Z_b and S parameters for the structures with wire and helix respectively.

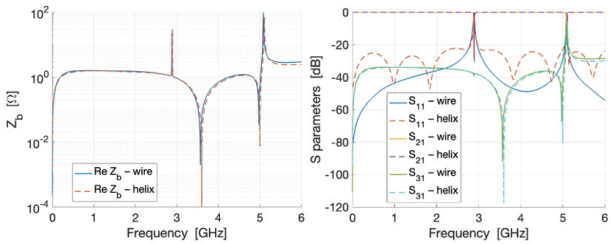

Figure 2: Left: transfer impedance comparison for the wire and helix structures, Right: different S-parameter comparison for wire and helix structures.

Figure 3 presents the real and imaginary parts of the longitudinal beam-coupling impedance $Z_{\parallel}(\omega)$ obtained from the wakefield simulation over the range 0-20 GHz. A broad inductive plateau is observed up to about 2.5 GHz; above this frequency a series of narrow resonances become visible. The first pronounced higher-order mode (HOM) appears at f ≃ 2.8 GHz with a peak impedance of ≈60 Ω. Higher modes at 4.8 GHz and 9.9 GHz exhibit successively lower coupling impedances.

To compare the wakefield results, the structure was also simulated with the classical stretched-wire method and with wire wrapped by a conducting helix to emulate subrelativistic field patterns. Figure 4 shows the real part of longitudinal beam coupling impedance up to first trapped

ISBN: 978-3-95450-262-2 ISSN: 2673-5350 doi: 10.18429/JACoW-IBIC2025-WEPMO30

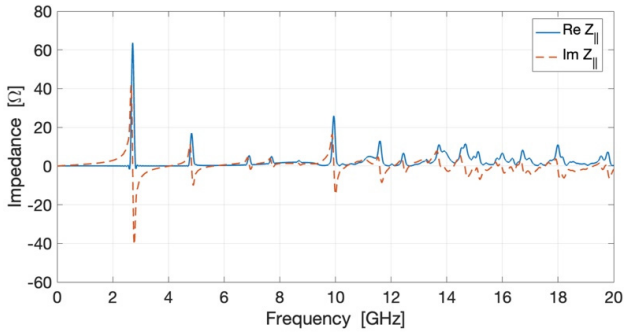

Figure 3: Real and imaginary parts of the beam coupling impedance.

higher order mode, 2.5 GHz on a logarithmic scale for:

- wakefield post-processing (solid blue),
- wire technique (dashed red).

The curves overlap within acceptable tolerance over the entire band.

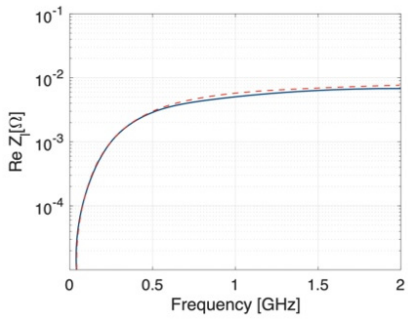

Figure 4: Comparison of real part of the beam coupling impedance calculated by wakefield simulations and from S-parameters.

Finally, Figure 5 displays a two-dimensional map of the BPM vertical Δ/Σ output voltage as a function of beam offset (–10 mm ≤ y ≤ 10 mm, The contours are nearly linear within ±4 mm.

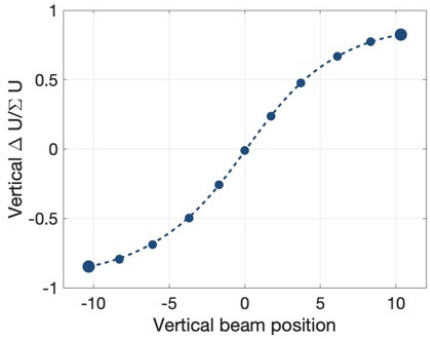

Figure 5: Reconstructed vertical beam position calculated using 'delta-over-sum' algorithm from signal registered in vertical buttons for zero horizontal beam displacement.

CONCLUSION

Presented designed for compact button-BPM for the KIU S2C2 beamline. Circuit analysis and 3D wake/S-parameter simulations indicate that a 14 mm button with 1 mm gap in a 25 mm radius of pipe delivers sufficient transfer impedance while keeping longitudinal impedance at reasonable level. $Z_{\parallel}$ is inductive to ≈2.5 GHz, with the first HOM near 2.8 GHz (~60 Ω). Wire/helix methods agree with wake results, validating the model. The Δ/Σ response is near-linear within ±4 mm and remains sensitive for 10^{-11}–10^{-10} C bunches, meeting the beamline requirements.

REFERENCES

[1] W. Kleeven *et al.*, "The IBA Superconducting Synchrocyclotron Project S2C2", in *Proc. Cyclotrons'13*, Vancouver, Canada, Sep. 2013, paper MO4PB02, pp. 115-119.

[2] E. Pearson *et al.*, "The new IBA superconducting synchrocyclotron (S2C2): From modeling to reality", in *Proc. Int. Topical Meet. Nucl. Appl. Accel.* (AccApp '13). Bruges, Belgium.

[3] F. Marcellini, M. Serio, A. Stella, and M. Zobov, "DAΦNE broad-band button electrodes", *Nucl. Instrum. Methods Phys. Res. A*, vol. 402, no. 1, pp. 27–35, Jan. 1998. doi:10.1016/s0168-9002(97)01083-8

[4] R.E. Shafer, "Beam position monitor sensitivity for low-β beams", *AIP Conf. Proc.*, vol. 319, pp. 303–308, 1994. doi:10.1063/1.46975

[5] R.E. Shafer, "Beam position monitoring". *AIP Conf. Proc.*, vol. 249, pp. 601-636, 1992. doi:10.1063/1.41980

[6] P. Kowina *et al.*, "FEM simulations – A powerful tool for BPM design", in *Proc. DIPAC'09,* Basel, Switzerland, paper MOOC03, pp. 35-37.

[7] S. Bilanishvili and M. Zobov, "Capacitive BPM electromagnetic design optimisation," *J. Phys. Conf. Ser.*, vol. 2687, no. 7, p. 072004, 2024. doi:10.1088/1742-6596/2687/7/072004

[8] P. Forck, P. Kowina, and D. Liakin, "Beam position monitors", *CAS – CERN Accelerator School: Beam Diagnostics,* CERN, pp. 187-228, 2009. doi:10.5170/CERN-2009-005.187

[9] M. Wendt, "BPM systems: A brief introduction to beam position monitoring", *arXiv*, 2018. doi:10.48550/arXiv.2005.14081

[10] M. Wang *et al.*, "Progress of low-β BPM calibration based on helical slow-wave structure", in *Proc. IBIC'24,* Beijing, China. Sep. 2024, pp. 142-144. doi:10.18429/JACoW-IBIC2024-TUP40

[11] ANSYS Inc. (n.d.). Ansys HFSS [Computer software]. https://www.ansys.com/products/electronics/ansys-hfss

[12] CST Studio Suite, Dassault Systèmes, https://www.cst.com/